

Cedric Jonathan C. Ng, MD¹
Ryan U. Chua, MD¹
Michael M. Laxamana, MD²

¹Department of Otorhinolaryngology
Head and Neck Surgery
University of Santo Tomas Hospital

²Department of Radiological Sciences
University of Santo Tomas Hospital

Correspondence: Dr. Ryan Uy Chua
Department of Otorhinolaryngology
Head and Neck Surgery
University of Santo Tomas Hospital
España Blvd, Sampaloc, Metro Manila 1015
Philippines
Phone: +63 917 554 7926
Email: ryanuychua@gmail.com

The authors declare that this represents original material, that the manuscript has been read and approved by the authors, that the requirements for authorship have been met by each author, and that the authors believe that the manuscript represents honest work.

Disclosure: The authors signed disclosures that there are no financial or other (including personal) relationships, intellectual passion, political or religious beliefs, and institutional affiliations that might lead to a conflict of interest.

Presented at the 2025 Singapore ENT-HNS Congress Oral Research Presentation Contest (3rd Place), Holiday Inn Atrium Singapore, April 6, 2025; and the Philippine Society of Otolaryngology-Head and Neck Surgery Descriptive Research Contest (1st Place), Natrapharm, Inc., Patriot Bldg., Parañaque City, August 15, 2025.

Data Sharing and Availability Statement: The datasets generated and analyzed in this study are available from the corresponding author upon request, subject to approval by the University of Santo Tomas Hospital – Research Ethics Committee.



Creative Commons (CC BY-NC-ND 4.0)
Attribution - NonCommercial - NoDerivatives 4.0 International

Mapping the Filipino Pediatric Skull Base: A Computed Tomography-Based Analysis of Anatomical Parameters and Nasoseptal Flap Reconstruction Feasibility from a Single Tertiary Hospital in the Philippines

ABSTRACT

Objective: To establish radiographic baseline measurements of key anatomical parameters of the Filipino pediatric skull base using computed tomography (CT); compare these anatomical parameters across different pediatric age groups and between sexes; and determine the feasibility of nasoseptal flap reconstruction for sellar defects in a Filipino pediatric population by calculating the nasoseptal flap to sellar defect length ratio (NSR).

Methods:

Design: Review of Records

Setting: Tertiary Academic Medical Center

Participants: Digital Imaging and Communications in Medicine (DICOM) images

of patients aged 0-17 years who had high-resolution head CT scans done at the University of Santo Tomas Hospital during the period of January 2019 – January 2024 were retrieved and reviewed. The following measurements were obtained: piriform aperture width (PAW), nare to sella distance (NSD), sphenoid to sella distance (SSD), sphenoid pneumatization type (SP), sphenoid sinus width (SW), olfactory fossa depth (OFD), lateral lamella cribriform plate angles (CPA), intercarotid distances (ICD) at the superior clivus (ICD-SC) and cavernous sinus (ICD-CS), potential nasoseptal flap length (NSF), potential sellar defect length (SDL) and nasoseptal flap length to sellar defect length ratio (NSR). Participants were stratified into three age groups (<5 years, 5-12 years, 13 years and older), and sex (males, females). Between-group comparisons were performed using ANOVA, chi-square and independent t-tests ($\alpha = 0.05$).

Results: Among the 111 participants (median age 12 years, IQR 7-15), 63.06% were males. For children <5 years ($n = 23$), mean values were: PAW 1.82 ± 0.15 cm, NSD 5.84 ± 0.37 cm, SSD 1.40 ± 0.35 cm, SW 1.78 ± 0.44 cm, OFD 0.53 ± 0.18 cm, ICD-SC 1.04 ± 0.20 cm, ICD-CS 1.64 ± 0.18 cm, NSF 4.95 ± 0.45 cm, and SDL 4.21 ± 0.64 cm. For ages 5-12 years ($n = 39$), values were: PAW 2.06 ± 0.23 cm, NSD 6.71 ± 0.50 cm, SSD 1.67 ± 0.24 cm, SW 2.55 ± 0.54 cm, OFD 0.61 ± 0.16 cm, ICD-SC 1.19 ± 0.21 cm, ICD-CS 1.86 ± 0.18 cm, NSF 5.63 ± 0.59 cm, and SDL 4.70 ± 0.85 cm. For ages ≥ 13 years ($n = 49$), values were: PAW 2.21 ± 0.26 cm, NSD 7.22 ± 0.63 cm,



SSD 1.86 ± 0.33 cm, SW 3.04 ± 0.66 cm, OFD 0.64 ± 0.23 cm, ICD-SC 1.23 ± 0.26 cm, ICD-CS 1.92 ± 0.24 cm, NSF 6.50 ± 0.50 cm, and SDL 5.59 ± 0.90 cm. Most participants had sellar-type sphenoid pneumatization ($n = 48, 43.24\%$) and Type 2 Keros classification ($n = 74, 66.67\%$). Sphenoid pneumatization differed significantly across age groups ($p = .001$), with conchal type predominant in <5 years ($n = 22, 95.65\%$), presellar in 5-12 years ($n = 18, 46.15\%$), and sellar in ≥ 13 years ($n = 38, 77.55\%$). The mean nasoseptal flap to sellar defect ratio (NSR) was 1.21 ± 0.22 overall and did not differ across age groups ($p = .677$), indicating adequate flap length for reconstruction across all ages.

Conclusion: In this sample, Filipino pediatric skull base anatomy demonstrates significant age-related dimensional changes but no sex-dependent differences. Despite smaller absolute dimensions in younger children, nasoseptal flap reconstruction appears radiographically feasible across all pediatric age groups. Our findings provide population-specific normative data to guide preoperative planning for pediatric endoscopic endonasal skull base surgery.

Keywords: *tomography, X-Ray computed; skull base; endoscopy; endoscopic surgical procedures; nasal septum; sphenoid sinus; reconstructive surgical procedures; anatomy, regional; child; transphenoidal surgery*

Skull base lesions in the pediatric population comprise a heterogeneous group of pathologies, including neural, mesenchymal, notochordal, vascular and epithelial origin.¹ While relatively uncommon and predominantly benign, these lesions may enlarge and exert significant mass effects, resulting in substantial morbidity that necessitates surgical intervention. In the Philippines, published data on pediatric skull base tumors remain limited. A 2021 review reported an incidence rate of 4.3 – 18.6 per 100,000 per year, with 2,297 cases and 1969 deaths.² Among these cases, 17.6% were untreated due to financial constraints as well as apprehensions that come with radical skull base surgical approaches.²

Endoscopic endonasal surgery (EES) has increasingly emerged as a viable and minimally invasive alternative to traditional open approaches in pediatric skull base surgery.^{3,4} However, pediatric skull base anatomy differs significantly from adults due to ongoing craniofacial development, variable sphenoid pneumatization, narrower intercarotid distances and piriform aperture width.^{4,9} In addition, endoscopic resection of skull base lesions often requires reconstruction of skull base defects with the use of vascularized tissue flaps – the most common of which is the pedicled nasoseptal flap.¹⁰ The literature on

nasoseptal flap reconstruction of pediatric skull base lesions is limited, with contradicting findings as to whether pediatric patients have adequate nasoseptal flap length for reconstruction.¹⁰⁻¹² Moreover, although international radiographic studies have characterized pediatric skull base parameters, there remains a paucity of population-specific anatomical data for Filipino children.^{4-9,13-15} A search of MEDLINE (PubMed), HERDIN Plus and Google Scholar revealed no studies on the radiographic measurements of pediatric skull base parameters or viability of nasoseptal flap reconstruction among Filipinos. This absence of locally derived normative measurements limits evidence-based surgical planning and risk stratification.

This study aims to establish radiographic baseline measurements of key anatomical parameters of the Filipino pediatric skull base using computed tomography (CT); compare these anatomical parameters across different pediatric age groups and between sexes; and determine the feasibility of nasoseptal flap reconstruction for sellar defects in a Filipino pediatric population by calculating the nasoseptal flap to sellar defect length ratio (NSR).

METHODS

With University of Santo Tomas Hospital Research Ethics Committee approval (Protocol Reference Number REC-2024-11-162-TR-AP), this review of records considered for inclusion pediatric high-resolution CT scans of the head obtained at the University of Santo Tomas Hospital from January 2019 to January 2024.

Inclusion criteria were age 0-17 years, DICOM files of head CT scans (e.g., craniofacial, maxillofacial, paranasal sinus, facial) with high resolution thin section (0.9 mm or less) CT images wherein each of the measurement parameters could be determined, with scans obtained as part of clinical evaluation for various indications unrelated to skull base pathology. Some of these included initial evaluations for craniofacial fractures, chronic rhinosinusitis, and preoperative planning for dental procedures, provided that no radiographic evidence of fracture or anatomical distortion was present. All scans were obtained using a GE Revolution™ Maxima 128-Slice Computed Tomography Machine (GE Healthcare, Cytiva Life Sciences, Global Life Sciences Solutions USA LLC, Wilmington DE USA).

Excluded were scans with confirmed craniofacial fractures, skull base trauma, prior skull base surgeries, and or congenital facial anomalies; those with radiographic evidence of tumors or lesions involving the maxillofacial region, sinonasal tract, maxilla, orbit, and or anterior skull base that distorted the normal pediatric anatomy; incomplete imaging of the paranasal sinuses and the anterior skull base region, including cuts that did not capture the entire nasoseptal or sphenoid area; and poor image quality due to motion artifacts, or

technical limitations (e.g., corrupted CT DICOM files) that impair clear visualization and measurement of critical structures such as the lateral lamella-cribriform plate angles, sphenoid sinus width, intercarotid distances, and sphenopalatine foramen.

Participants were stratified into three age groups: <5 years, 5-12 years, and ≥ 13 years. This classification was based on established patterns of craniofacial development: early maturation and rapid development of the cranial base occurs during early childhood (ages <5 years), followed by a period of relatively fixed growth (ages 5-12 years), and minimal growth which occurs from age 13 years onward.⁴ This tiering allows for age-specific surgical planning and identification of anatomical limitations that may impact the feasibility and safety of endoscopic approaches.

All measurements were performed independently by the otolaryngologist authors using Radiant DICOM medical image viewer (Version 2025.1, Medixant, Poznań, Poland) and cross-checked by a board-certified radiologist co-author. Final confirmed measurements were used for analysis. Multiplanar views (axial, coronal, and sagittal) were evaluated in bone window settings (width 2000, level 350). All linear measurements were expressed in centimeters (cm) and angles in degrees ($^{\circ}$). Measurement landmarks followed standardized protocols established in prior literature^{4,10} to ensure reproducibility.

Figures 1-5 are representative images of the measurements used in this study. Measurements and landmarks were similar to those used by Chen *et al.*⁴ and Purcel *et al.*¹⁰ for standardization. **Piriform aperture width (PAW)** was measured in the coronal plane of the CT scan. (Figure 1A) **Nare to Sella Distance (NSD)** was measured from the anterior tip of the nasal aperture to anterior wall of sphenoid sinus in the midsagittal plane. (Figure 1B) **Sphenoid to Sella Distance (SSD)** was measured as the distance from the anterior wall of the sphenoid to the floor of the sella. (Figure 1C) **Sphenoid sinus width (SW)** was measured as the widest points in the coronal cut within the pneumatized sphenoid sinus. (Figure 1D) The **depth of the olfactory fossa (OFD)** was measured by acquiring the height of the cribriform plate to the inferior aspect of the fovea ethmoidalis, as described by Keros.¹⁶ (Figure 1E) For this parameter – where asymmetry may be present between sides – the longer depth was consistently recorded, identical to the methodology of Chen and colleagues⁴ for standardization. This was also chosen by the authors to reflect the more vulnerable side in terms of potential surgical risk and anatomical limitation, particularly relevant in pediatric endoscopic skull base procedures. The **intercarotid distances (ICD)** were measured at the level of the superior **clivus (ICD-SC)** and **cavernous sinus (ICD-CS)** in the axial plane. The **ICD-SC** was measured as the minimum distance between medial aspects of the carotid canals at the SC inferior to the sellar floor. (Figure 2A) The **ICD-CS** was measured as the minimum

distance between medial aspects of the carotid prominence within the CS above the sellar floor. (Figure 2B) **Sphenoid sinus pneumatization (SP)** was classified and divided into three groups as had been done by Chen *et al.*⁴ – conchal, presellar and sellar types. The conchal type was defined as the sella turcica (ST) completely surrounded by bone, and sinus aeration not reaching the anterior sellar wall (ASW). (Figure 3A) The presellar type was defined as the anterior half of the sella being exposed to air, with the posterior-most aspect of the sella ending at the ASW. (Figure 3B) Lastly, the sellar type was defined as the sinus extending past the ASW. (Figure 3C) The **Cribriform Plate angle (CPA)** was measured in the coronal plane, as the angle between the lateral lamella and the cribriform plate on each side – left and right. (Figure 4A and B) Potential **nasoseptal flap length (NSF)** was measured as the linear distance from the sphenopalatine foramen to the nasal sill in the midsagittal plane. (Figure 5A) Potential **sellar defect length (SDL)** was measured as the curvilinear distance from the sphenopalatine foramen to the posterior planum sphenoidale in the midsagittal plane. (Figure 5B) Lastly, the **nasoseptal flap length to sellar defect length ratio (NSR)** was calculated as the ratio of NSF and SDL. A ratio of greater than or equal to 1 indicated that the potential nasoseptal flap length would be sufficient for the potential sellar defect length, and thus, nasoseptal flap reconstruction would be feasible,¹⁰ while a ratio of less than 1 indicated otherwise.

Data Analysis

Statistical analyses were conducted using STATA MP-Parallel Version Statistical Software, Version 18 (StataCorp LLC, College Station, TX, USA). Descriptive statistics reported means and standard deviations for normally distributed, continuous data; medians and interquartile ranges for ordinal and non-normally distributed data; and frequencies and percentages for categorical variables. Data normality was analyzed using Shapiro-Wilk's Test. The pediatric maxillofacial anatomical parameters (PAW, NSD, SSD, SP, SW, OFD, CPA-R, CPA-L, ICD-SC, ICD-CS, NSF and SDL) were reported using means and standard deviations and frequencies and percentages, depending on the level of data measurement alongside their respective 95% confidence intervals (CI). Between-group comparisons according to sex (males vs. females) and age groups (<5 years old, 5 to 12 years old, vs. ≥ 13 years old) were conducted using the Chi-Square of homogeneity for categorical variables; the Mann-Whitney U or Kruskal-Wallis H Test for ordinal or non-normal, continuous variables; and independent t-test or one-way analysis of variance (ANOVA) for normally-distributed, continuous variables. For between-group comparisons according to age group which were statistically significant, *post hoc* pairwise comparisons using Bonferroni adjustments were conducted. A *p*-value of $\leq .05$ was considered statistically significant.



RESULTS

Of the 135 DICOM files initially considered for inclusion, 24 CT scans were excluded because of the following reasons: facial fractures (eight scans), radiologic evidence of maxillofacial tumors (five scans), radiologic evidence of cranial/skull base tumors (six scans), and corrupted DICOM files (five), yielding a final sample of 111 participant records. *Post hoc* power analysis showed that the acquired sample was sufficient.

Most of the participants were males ($n = 70$; 63.06%). Their median age was 12 years old (IQR 7.00 – 15.00). Of these, 23 (20.72%) were < 5 years, 39 (35.14%) aged 5-12 years, and 49 (44.14%) were ≥ 13 years old.

Table 1 shows the pediatric maxillofacial parameters among the participants. The mean PAW, NSD, SSD, SW, and OFD were 2.07 cm (SD = 0.28), 6.75 cm (SD = 0.75), 1.70 cm (SD = 0.35), 2.61 cm (SD = 0.74), and 0.61 cm (SD = 0.20), respectively. The mean lateral lamella CPA right and left were 114.25° (SD = 9.92) and 111.02° (SD = 8.81), respectively. The mean ICD-SC was 1.17 cm (SD = 0.24), the mean ICD-CS was 1.84 cm (SD = 0.23), the mean NSF was 5.87 cm (SD = 0.81), and the mean SDL was 4.99 cm (SD = 1.00). The mean nasoseptal flap length to sellar defect length ratio was 1.21 (SD = 0.22). Most of the participants had a sellar type of sphenoid pneumatization ($n = 48$, 43.24%) and a type 2 Keros classification ($n = 74$, 66.67%).

A one-way ANOVA conducted to compare anatomical measurements across age groups (<5 years, 5-12 years, ≥ 13 years) showed significant age-related differences in the following: PAW ($F[2,108] = 27.77$, $p = .001$), NSD ($F[2,108] = 50.87$, $p = .001$), SSD ($F[2,108] = 17.57$, $p = .001$), SW ($F[2,108] = 36.47$, $p = .001$), ICD-SC ($F[2,108] = 5.29$, $p = .053$), ICD-CS ($F[2,108] = 14.68$, $p = .001$), NSF ($F[2,108] = 74.63$, $p = .001$), and SDL ($F[2,108] = 24.98$, $p = .001$). Table 2 depicts the comparative analyses of the pediatric maxillofacial parameters according to age groups. Univariate analysis showed that PAW, NSD, SSD, SW, ICD-SC, ICD-CS, NSF, and SDL were statistically different among the three age groups ($p < .05$). For the PAW, NSD, SSD, SW, and NSF, Bonferroni adjustments indicated that the mean scores were significantly higher among those who were ≥ 13 years old and were significantly lowest among those <5 years old. In terms of ICD-SC, results showed that the mean ICD-SC of those who were ≥ 13 years old was significantly higher compared to those who were <5 years old ($p = .005$), while other pairwise comparisons were not statistically different ($p > .05$). For ICD-CS, the mean ICD-CS among those <5 years old was significantly lower than those who were 5 to 12 years old ($p = .001$) and ≥ 13 years old ($p = .001$). However, the mean ICD-CS between 5 to 12 years old and ≥ 13 years old were not statistically different ($p = .510$). The mean SDL among those who were ≥ 13 years old was significantly higher compared to those who were <5 years old ($p = .001$) and those who were 5 to 12 years old ($p = .001$). The

mean SDL between those who were <5 years old and 5 to 12 years old were not statistically different ($p = .087$). It can also be gleaned from the table that the mean NSR was not significantly different across the age groups ($F[2,108] = 0.39$, $p = .677$).

On the other hand, a chi-square test of homogeneity performed to evaluate whether sphenoid sinus pneumatization patterns differed across age groups also showed that the proportion of the different sphenoid pneumatization types were significantly different across the age groups ($\chi^2[4, N = 111] = 81.75$, $p = .001$), while the Keros classification were not ($\chi^2(4, N = 111) = 2.79$, $p = .605$). The conchal type was significantly higher among those <5 years old (95.65% vs. 28.21% vs. 2.04%), while the presellar type was significantly prevalent among those who were 5 to 12 years old. In addition, the sellar type was significantly higher among those who were ≥ 13 years old.

Independent samples t-tests to compare pediatric maxillofacial parameters according to sex are illustrated in Table 3. The mean NSD, SW, OFD, CPA on both right and left areas, ICD-SC, ICD-CS, NSF, and SDL showed higher values among males while the mean PAW and SSD values were greater among females. Nevertheless, the comparisons of these parameters according to sex were not statistically significant. Indeed, no statistically significant sex-based differences were identified in: PAW ($t[109] = -0.16$, $p = .872$), NSD ($t[109] = 1.71$, $p = .090$), SSD ($t[109] = -0.37$, $p = .709$), SW ($t[109] = 1.39$, $p = .167$), ICD-SC ($t[109] = 0.89$, $p = .377$), ICD-CS ($t[109] = 0.26$, $p = .797$), NSF ($t[109] = 1.75$, $p = .083$), and SDL ($t[109] = 0.71$, $p = .479$). It can also be noted that the proportions of a sellar type of sphenoid pneumatization was most prevalent in both males ($n = 32$, 45.71%) and females ($n = 16$, 39.02%), but these were not statistically different ($\chi^2[2, N = 111] = 2.17$, $p = .375$). Similarly, a Type 2 Keros was most prevalent on both sexes (males: $n = 45$, 64.29%, females: $n = 29$, 70.73%), but were not significantly different as well ($\chi^2[2, N = 111] = 2.65$, $p = .264$). The mean NSR were also higher among males ($\bar{x} = 1.21$, SD = 0.21) than females ($\bar{x} = 1.20$, SD = 0.23) but were not significantly different between sexes ($t[109] = 0.42$, $p = .667$).

DISCUSSION

Our study established radiographic baseline measurements of key anatomical parameters of the pediatric skull base in a Filipino population and evaluated their variation across age groups and sex. We found that most parameters – including PAW, NSD, SSD, SW, ICD-SC, ICD-CS, NSF and SDL – increased significantly with age, whereas no statistically significant sex-based differences were observed. Sphenoid pneumatization also demonstrated a clear developmental progression from predominantly conchal type in children younger than 5 years to sellar type in adolescents. These findings reflect the developmental progression of the pediatric skull base. Early childhood (<5 years

Table 1. Descriptive Statistics of Pediatric Maxillofacial Parameters (N = 111)

Maxillofacial Pediatric Parameters	Mean (SD)	Frequency (%)	95% CI
PAW (cm; \bar{x}, SD)	2.07 (0.28)		2.02 – 2.12
NSD (cm; \bar{x}, SD)	6.75 (0.75)		6.61 – 6.89
SSD (cm; \bar{x}, SD)	1.70 (0.35)		1.63 – 1.76
SP (f, %)			
Conchal		34 (30.63)	22.23 – 40.09
Presellar		29 (26.13)	18.25 – 35.32
Sellar		48 (43.24)	33.87 – 52.98
SW (cm; \bar{x}, SD)	2.61 (0.74)		2.47 – 2.75
OFD (cm; \bar{x}, SD)	0.61 (0.20)		0.57 – 0.64
Keros Classification (f, %)			
Type 1		18 (16.22)	9.90 – 24.41
Type 2		74 (66.67)	57.09 – 75.33
Type 3		19 (17.12)	10.63 – 25.43
CPA ($^{\circ}$; \bar{x}, SD)			
Right	114.25 (9.92)		112.39 – 116.12
Left	111.02 (8.81)		109.36 – 112.68
ICD-SC (cm; \bar{x}, SD)	1.17 (0.24)		1.13 – 1.22
ICD-CS (cm; \bar{x}, SD)	1.84 (0.23)		1.80 – 1.89
NSF (cm; \bar{x}, SD)	5.87 (0.81)		5.72 – 6.02
SDL (cm; \bar{x}, SD)	4.99 (1.00)		4.80 – 5.18
NSR (\bar{x}, SD)	1.21 (0.22)		1.17 – 1.25

Abbreviations: PAW = Piriform Aperture Width (PAW); NSD = Nare to Sella Distance; SSD = Sphenoid to Sella Distance; SP = Sphenoid Pneumatization Type; SW = Sphenoid Sinus Width; OFD = Olfactory Fossa Depth; CPA = Lateral Lamella Cribriform Plate Angles; ICD-SC = Intercarotid Distances at the Superior Clivus; ICD-CS = Intercarotid Distances at the Cavernous Sinus; NSF = Nasoseptal Flap Length; SDL = Sellar Defect Length; NSR = Nasoseptal Flap Length to Sellar Defect Length Ratio

group) represents the period of rapid skull base development and incomplete sphenoid pneumatization. Late childhood (5-12 years group) represents a transition phase with progressive pneumatization and stable but ongoing growth. By adolescence (≥ 13 years group), many skull base structures approach near-adult anatomy with completed or near-completed sphenoid pneumatization.^{4,6,17-19} These developmental changes help explain the progressive increase in anatomical dimensions observed across age groups and highlight the importance of age-specific considerations in pediatric EES. Importantly, despite age-related dimensional changes, the NSR remained stable and greater than 1 across all age groups, suggesting consistent reconstructive feasibility throughout pediatric development. Because this was a retrospective study, an *a priori* sample size calculation was not performed. A *post hoc* power analysis using G*Power Version 3.1.9.4 (Heinrich Heine University, Düsseldorf, Germany) was conducted based on the observed multivariate effect size. Using a Pillai's V of 0.1967, corresponding to an effect size $f^2(V)$ of 0.2449, with six groups, two predictors, fourteen outcomes, and an alpha level of 0.05, the achieved statistical power was estimated at 0.995. This suggests that the final

sample of 111 participants was adequate to detect the observed age-related differences in anatomical parameters. However, because *post hoc* power is inherently derived from the observed effect size, it should be interpreted cautiously and does not substitute for prospective sample size estimation.

The anterior nasal (piriform) aperture is the most superficial bony structure encountered during nasal endoscopy, and is the first limitation in endoscopic surgery as it constricts lateral movement of surgical instruments, and consequently limits lateral dissection as well. According to the literature, PAW of greater than 2 cm provides unrestricted access for endoscopic surgery, while less than 1.5 cm may be insufficient.⁴ Our study shows that the mean PAW among Filipino pediatric patients was 2.07 cm (20.7 mm), which is similar to previous studies done elsewhere.^{4,9} A closer look into the width across age groups show that PAW is significantly different across groups which suggests an increase in PAW as age increases. These findings suggest that surgical instrument maneuverability improves with age, although even younger cohorts may still permit endoscopic access with appropriately sized instrumentation. The PAW across sexes were not statistically significant which implies that the sex of the patient will not affect the surgeon's approach to EES. Tatreau and colleagues⁹ have measured the PAW among pediatric and adult patients, with PAW findings among adult patients that range from 20.9 – 23.6 mm. This finding, juxtaposed with the findings of our study suggests that the PAW among Filipino pediatric patients (aged 5 onwards) does not relatively differ compared to adults. (Table 4)

Nare to sella distance is the distance required to access the anterior part of the sellar compartment, which is a crucial measurement point for endonasal transsphenoidal approaches. Studies have shown that NSD among pediatric patients can range from 6.10 – 7.88 cm.⁴ Our study shows a mean NSD of 6.75 cm, which is well within the range specified. Comparing the NSD between age groups showed that the values were statistically significant. This means that NSD increases as the age of the patient increases as well. This is consistent with the findings presented in previous literature.^{4,9} Interestingly, previous studies have shown that NSD is sex dependent, with females having smaller NSD compared to males.^{4,19} Our current study, however, shows otherwise. The NSD among Filipino pediatric males (6.85 cm) vis-à-vis females (6.60 cm) did not statistically differ.

Sphenoid to sella distance is another important parameter in ESS. This determines how far the surgeon is from the sellar compartment when the anterior wall of the sphenoid sinus has been accessed. Our study shows that the mean SSD among Filipino children is about 1.70 cm, which is relatively smaller when compared to the study done by Sawant *et al.*¹⁷ Based on the measurements of Sawant,¹⁷ the

**Table 2.** Between-Group Comparisons of the Maxillofacial Pediatric Parameters among the Participants according to Age Group (N = 111)

Maxillofacial Pediatric Parameters	Age Group (N = 111)			Overall p-value (Two-Tailed)	Pairwise Comparisons ^a		
	<5 Years Old (n = 23)	5 to 12 Years Old (n = 39)	≥13 Years Old (n = 49)		<5 Years Old vs. 5 to 12 Years Old	<5 Years Old vs. ≥13 Years Old	5 to 12 Years Old vs. ≥13 Years Old
PAW (cm; \bar{x}, SD)	1.78 (0.15)	2.06 (0.23)	2.21 (0.26)	.001*	0.001*	0.001*	0.008*
NSD (cm; \bar{x}, SD)	5.84 (0.37)	6.71 (0.50)	7.22 (0.63)	.001*	0.001*	0.001*	0.001*
SSD (cm; \bar{x}, SD)	1.40 (0.35)	1.67 (0.24)	1.86 (0.33)	.001*	0.004*	0.001*	0.015*
SP (f, %)				.001*			
Conchal	22 (95.65%)	11 (28.21%)	1 (2.04%)		0.001*	0.001*	0.001*
Presellar	1 (4.35%)	18 (46.15%)	10 (20.41%)		0.001*	0.001*	0.394
Sellar	0 (0.00%)	10 (25.64%)	38 (77.55%)		0.008*	0.055	0.001*
SW (cm; \bar{x}, SD)	1.78 (0.44)	2.55 (0.54)	3.04 (0.66)	.001*	0.001*	0.001*	0.001*
OFD (cm; \bar{x}, SD)	0.53 (0.18)	0.61 (0.16)	0.64 (0.23)	.095	0.343	0.094	1.000
Keros Classification (f, %)				.605			
Type 1	4 (17.39%)	4 (10.26%)	10 (20.41%)		0.419	0.763	0.196
Type 2	16 (69.57%)	29 (74.36%)	29 (59.18%)		0.683	0.396	0.136
Type 3	3 (13.04%)	6 (15.38%)	10 (20.41%)		0.801	0.448	0.543
CPA (°; \bar{x}, SD)							
Right	114.10 (8.99)	115.46 (8.91)	113.36 (11.13)	.616	1.000	1.000	0.982
Left	108.13 (7.19)	113.22 (8.98)	110.64 (9.08)	.082	0.084	0.768	0.508
ICD-SC (cm; \bar{x}, SD)	1.04 (0.20)	1.19 (0.21)	1.23 (0.26)	.006*	0.053	0.005*	1.000
ICD-CS (cm; \bar{x}, SD)	1.64 (0.18)	1.86 (0.18)	1.92 (0.24)	.001*	0.001*	0.001*	0.510
NSF (cm; \bar{x}, SD)	4.95 (0.45)	5.63 (0.59)	6.50 (0.50)	.001*	0.001*	0.001*	0.001*
SDL (cm; \bar{x}, SD)	4.21 (0.64)	4.70 (0.85)	5.59 (0.90)	.001*	0.087	0.001*	0.001*
NSR (\bar{x}, SD)	1.20 (0.22)	1.23 (0.23)	1.19 (0.20)	.677	1.000	1.000	1.000

Abbreviations: SD = Standard Deviation; PAW = Piriform Aperture Width (PAW); NSD = Nare to Sella Distance; SSD = Sphenoid to Sella Distance; SP = Sphenoid Pneumatization Type; SW = Sphenoid Sinus Width; OFD = Olfactory Fossa Depth; CPA = Lateral Lamella Cribriform Plate Angles; ICD-SC = Intercarotid Distances at the Superior Clivus; ICD-CS = Intercarotid Distances at the Cavernous Sinus; NSF = Nasoseptal Flap Length; SDL = Sellar Defect Length; NSR = Nasoseptal Flap Length to Sellar Defect Length Ratio

^aNote: Values are presented as p-values

*Significant at 0.05

average sphenosellar distance among Indian patients was shown to be ranging from 1.73 – 2.06 cm. Measurements across age groups were statistically different as well, similar to the findings seen in our study. A reduced SSD in Filipino pediatric patients suggests a tighter corridor between the nasal cavity and the sella. Surgeons must anticipate a slightly narrower working space and consider the use of smaller-caliber angled endoscopes (2.7 or 3 mm) and instruments during transsphenoidal approaches. Nevertheless, the progressive increase in NSD and SSD across age reflects elongation of the anterior skull base and maturation of the sphenoid sinus, findings that parallel those in literature.^{4,17} (Table 4)

Sphenoid pneumatization demonstrated a marked age-dependent pattern, with nearly all children younger than 5 years exhibiting conchal pattern, while older children predominantly showed sellar type of pneumatization. This progression mirrors established developmental patterns described in pediatric skull base studies.^{4,20} Although incomplete pneumatization may increase operative complexity due to additional drilling requirements, Kuan and colleagues have determined that incomplete pneumatization is not a contraindication to endonasal surgery.²⁰ Our findings support this perspective and emphasize that anatomical maturation, rather than categorical pneumatization type

alone, should inform surgical planning.

Sphenoid sinus width (SW) determines the visibility and working area for endoscopic surgery, which also corresponds to the lateral aeration of the sphenoid sinus. A greater SW value means decreased drilling and manipulation, improved visualization, and better surgical working area. Our study shows a mean SW of 2.61 cm with the following means across age groups: 1.78 (for less than 5 years), 2.55 (for 5-12 years), and 3.04 (for 13 years and older). The mean SW of our study is smaller compared to the average SW among adults (3.77 cm).²¹ The means across age groups were statistically significant, and this data agrees with the findings in the literature.⁴ The SW means however is not statistically different across sexes.

The olfactory fossa is the most inferomedial portion of the anterior cranial fossa harboring the olfactory nerve and bulb. It has a variable depression in the cribriform plate. The lateral lamella of the cribriform plate is the thinnest bone in the anterior skull base, and is most vulnerable for iatrogenic complications during endoscopic surgeries. The OFD in our study was measured from the cribriform plate to the fovea ethmoidalis as described by Keros.¹⁶ A greater OFD would mean a higher risk for injury. Subsequently, these measurements were then categorized accordingly based on the Keros classification, with type

Table 3. Comparisons of Pediatric Maxillofacial Parameters according to Sex (N = 111)

Maxillofacial Pediatric Parameters	Sex (N = 111)		p-value (Two-Tailed)
	Male, n = 70	Female, n = 41	
PAW (cm; \bar{x}, SD)	2.06 (0.29)	2.07 (0.26)	.873
NSD (cm; \bar{x}, SD)	6.85 (0.79)	6.60 (0.64)	.090
SSD (cm; \bar{x}, SD)	1.69 (0.37)	1.71 (0.30)	.709
SP (f, %)			.375
Conchal	23 (32.86%)	11 (26.83%)	
Presellar	15 (21.43%)	14 (34.15%)	
Sellar	32 (45.71%)	16 (39.02%)	
SW (cm; \bar{x}, SD)	2.68 (0.76)	2.48 (0.71)	.167
OFD (cm; \bar{x}, SD)	0.63 (0.20)	0.56 (0.18)	.076
Keros Classification (f, %)			.264
Type 1	10 (14.29%)	8 (19.51%)	
Type 2	45 (64.29%)	29 (70.73%)	
Type 3	15 (21.43%)	4 (9.76%)	
CPA (°; \bar{x}, SD)			
Right	114.68 (10.46)	113.53 (9.02)	.560
Left	111.04 (9.46)	110.99 (7.72)	.978
ICD-SC (cm; \bar{x}, SD)	1.19 (0.24)	1.15 (0.24)	.377
ICD-CS (cm; \bar{x}, SD)	1.85 (0.22)	1.84 (0.24)	.797
NSF (cm; \bar{x}, SD)	5.97 (0.85)	5.70 (0.70)	.083
SDL (cm; \bar{x}, SD)	5.04 (1.02)	4.90 (0.97)	.479
NSR (\bar{x}, SD)	1.21 (0.21)	1.20 (0.23)	.677

Abbreviations: SD = Standard Deviation; PAW = Piriform Aperture Width (PAW); NSD = Nare to Sella Distance; SSD = Sphenoid to Sella Distance; SP = Sphenoid Pneumatization Type; SW = Sphenoid Sinus Width; OFD = Olfactory Fossa Depth; CPA = Lateral Lamella Cribriform Plate Angles; ICD-SC = Intercarotid Distances at the Superior Clivus; ICD-CS = Intercarotid Distances at the Cavernous Sinus; NSF = Nasoseptal Flap Length; SDL = Sellar Defect Length; NSR = Nasoseptal Flap Length to Sellar Defect Length Ratio

aNote: Values are presented as p-values.

*Significant at 0.05

3 as the most dangerous. Findings of our study show that the mean OFD among Filipino pediatric patients is 0.61 cm, or a Keros type 2, with OFD being slightly higher among males (0.63 cm) but is not statistically significant across sex and age groups. Compared to the measurements of Chen and colleagues which showed a mean OFD of 0.28 cm (Keros type 1)⁴ as well as the measurements of Nair and Ibrahim which showed a mean OFD of 0.34 cm (Keros type 1),²² the OFD in our study is relatively higher, but is consistent with the radio-anatomical study done in *Türkiye*, where majority of the pediatric patients presented with a Keros type 2.²³ These findings suggest that OFD may vary across regions or race.

The lateral lamella-cribriform plate angle (CPA) is also an important aspect of the anterior cranial fossa as an obtuse angle would be more prone to injury than acutely angled one. In patients with obtuse CPA, surgeons may need to adjust the trajectory of instruments more horizontally, rather than vertically, to avoid sliding injuries. Studies on the CPAs are relatively limited, however, Nair and Ibrahim²² have argued that the angle of the lateral lamella in relation to the cribriform plate should be considered during pre-operative planning given that clinically, access to the skull base during routine EES is lateral to the middle turbinate. Their study classified CPAs into 3: type A (up to 120°), type B (120°–150°) and type C (150°–180°).²² The most common type in their study was Type A, followed by Type B, then Type C.²² Our study showed that mean CPAs are 114.25° and 111.02° for right and left respectively, all of which fall under the Type A classification. Despite the means not being significantly different across sex and age groups, we

Table 4. Comparison of the Means of Maxillofacial Pediatric Parameters of the Current Study with the Literature

Maxillofacial Pediatric Parameters	Ng et al. (2025)	Chen et al. (2022) ^a	Tatreau et al. (2010) ⁹	Sawant et al. (2020) ¹⁷	Banu et al. (2013) ¹⁹	Güven et al. (2021) ²³	Nair and Ibrahim (2020) ²²	Purcell et al. (2015) ¹⁰	Ghosh et al. (2015) ²⁵	Shah et al. (2009) ¹²
PAW (cm; \bar{x}, SD)	2.07 (0.28)	1.94 (0.26)	1.96 (0.18)							
NSD (cm; \bar{x}, SD)	6.75 (0.75)	6.99 (0.67)			7.58 (2.51)					
SSD (cm; \bar{x}, SD)	1.70 (0.35)			1.95 (0.29)						
SW (cm; \bar{x}, SD)	2.61 (0.74)	2.64 (1.29)								
OFD (cm; \bar{x}, SD)	0.61 (0.20)	0.28 (0.15)				0.47 (0.17)	0.34 (0.10)			
CPA (°; \bar{x}, SD)										
Right	114.25 (9.92)	118.2 (2.2)					117.9 (10.8)			
Left	111.02 (8.81)	119.6 (2.2)					119.4 (10.1)			
ICD-SC (cm; \bar{x}, SD)	1.17 (0.24)	1.62 (0.33)	1.99 (0.34)	1.45 (0.24)						
ICD-CS (cm; \bar{x}, SD)	1.84 (0.23)	1.07 (0.28)	1.08 (0.18)	1.67 (0.27)						
NSF (cm; \bar{x}, SD)	5.87 (0.81)								6.75 (0.98)	5.01 (0.32)
SDL (cm; \bar{x}, SD)	4.99 (1.00)								4.86 (0.78)	5.05 (0.55)
NSR (\bar{x}, SD)	1.21 (0.22)							1.47 (0.33)	1.39*	0.99*

Abbreviations: PAW = Piriform Aperture Width (PAW); NSD = Nare to Sella Distance; SSD = Sphenoid to Sella Distance; SP = Sphenoid Pneumatization Type; SW = Sphenoid Sinus Width; OFD = Olfactory Fossa Depth; CPA = Lateral Lamella Cribriform Plate Angles; ICD-SC = Intercarotid Distances at the Superior Clivus; ICD-CS = Intercarotid Distances at the Cavernous Sinus; NSF = Nasoseptal Flap Length; SDL = Sellar Defect Length; NSR = Nasoseptal Flap Length to Sellar Defect Length Ratio

***- The reported measurement represents a calculated value based on the available data and was not obtained from the literature. This is for the purpose of comparison only.

found that the *right* side is slightly more angulated than the *left* among Filipinos. This finding contrasted with the results of Nair and Ibrahim, wherein they found that the *left* side is more angulated than the *right*.²² Despite the CPA among the Filipino pediatric skull base being less angled, this does not mean that it does not come without any potential complications. Indeed, a more acute CPA corresponds to a steeper, more vertically oriented lateral lamella. This configuration places the cribriform plate closer to the surgical field, especially during superior ethmoid dissection. Instruments, when introduced more superiorly, are more likely to strike the skull base directly, increasing the risk of CSF leak or intracranial entry. These findings highlight the importance of CPA assessment in preoperative planning, especially when dealing with pediatric patients where skull based anatomy is less robust. Surgeons should consider modifying their dissection technique, adjusting instrument trajectory and may consider usage of navigation tools to reduce risk in cases with more obtuse cribriform plate angles.

The internal carotid artery typically determines the lateral limit of dissection in endoscopic surgery. Indeed, a narrow intercarotid distance is a relative contraindication to EES. Previous studies have stated that ICD-CS of less than 1 cm is particularly disadvantageous for EES,^{4,7,9} while an average ICD of 1.2 – 1.8 cm is accepted as normal.^{17,24} Our study showed a mean ICD-SC of 1.17, and ICD-CS of 1.84. Both are significantly different across age groups. These values increase with age, reflecting growth and expansion of the skull base. For ICD-SC, results showed that the mean ICD-SC of those who were ≥ 13 years old was significantly higher compared to those who were < 5 years old ($p = .005$), while other pairwise comparisons were not statistically different ($p > .05$). For ICD-CS, the mean ICD-CS among those < 5 years old was significantly lower than those who were 5 to 12 years old ($p = .001$) and ≥ 13 years old ($p = .001$). However, the mean ICD-CS between 5 to 12 years old and ≥ 13 years old were not statistically different ($p = .510$). Similar age-dependent widening of intercarotid corridors has been described in pediatric skull base analyses by Chen *et al.*⁴ and Banu *et al.*¹⁹ However, even in the youngest cohort, mean ICD values still fall within ranges previously reported in pediatric populations.^{4,24} Younger children demonstrated narrower measurements, which may theoretically increase technical difficulty during transclival or parasellar approaches. Smaller ICDs may also limit access for large instruments, endoscopes or even reconstructive flaps and may necessitate alternative approaches or delayed interventions in cases involving large defects or lesions. Minor variations between our measurements and those reported in other populations may reflect ethnic craniofacial differences or methodological variability, although such explanations remain hypothetical and warrant further investigation.

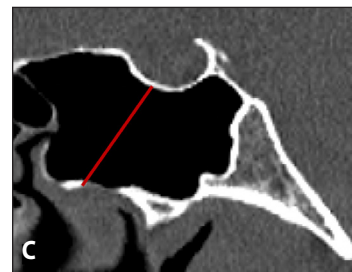
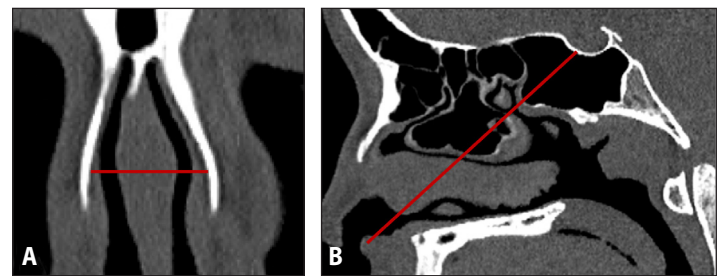


Figure 1. Anterior Skull Base Measurements: **A.** Piriform Aperture Width (PAW); **B.** Nare to Sella Distance (NSD); **C.** Sphenoid to Sella Distance (SSD); **D.** Sphenoid Sinus Width (SW); and **E.** Olfactory Fossa Depth (OFD)

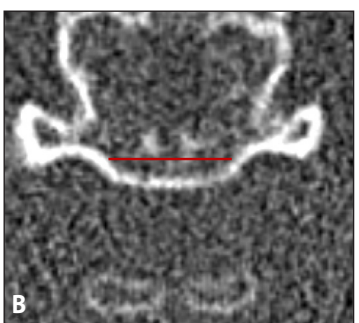
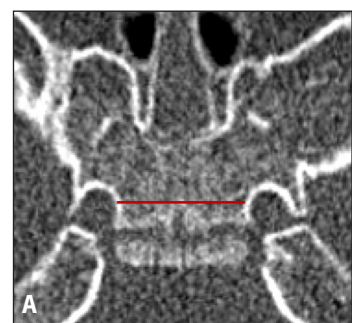
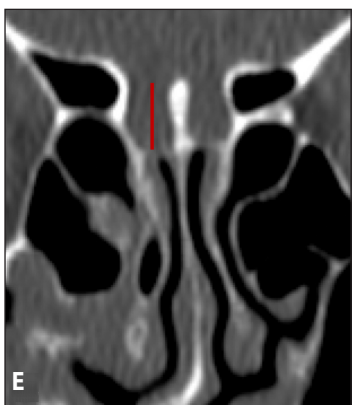
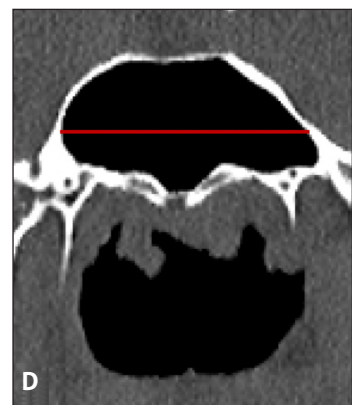


Figure 2. Intercarotid Distances at Different Skull Base Levels: **A.** Intercarotid distance at the superior clivus (ICD-SC); and **B.** Intercarotid distance at the cavernous sinus (ICD-CS)

With regards to reconstruction, the stability of NSR across age groups represents a clinically meaningful finding. Although both nasoseptal flap length and sellar defect length increased significantly with age, their proportional relationship still remained preserved, resulting in NSR values consistently exceeding 1.0. This finding suggests that reconstructive feasibility is maintained throughout pediatric development. Our findings contrasted with earlier concerns raised by Shah *et al.*¹² regarding inadequate flap length in younger children,

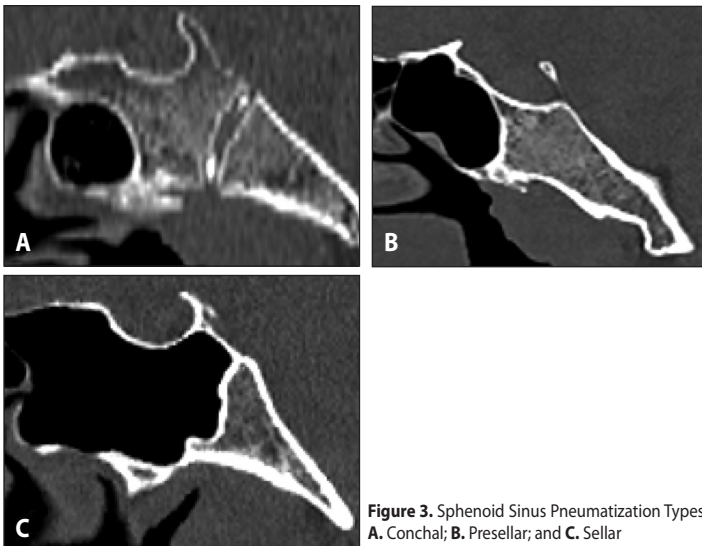


Figure 3. Sphenoid Sinus Pneumatization Types: **A.** Conchal; **B.** Presellar; and **C.** Sellar

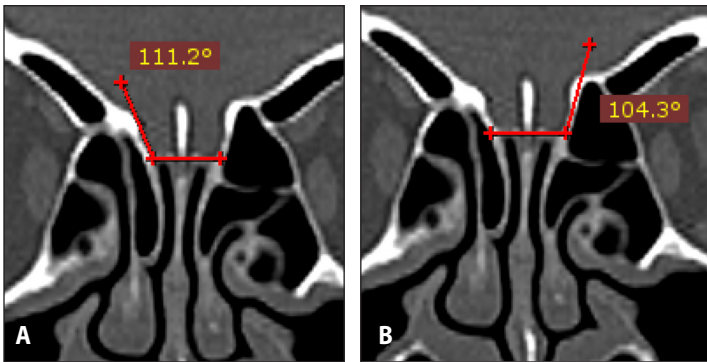


Figure 4. Lateral Lamella-Cribriform Plate Angles: **A.** Lateral Lamella – Cribriform Plate Angle, Right (CPA-R); and **B.** Lateral Lamella – Cribriform Plate Angle, Left (CPA-L)

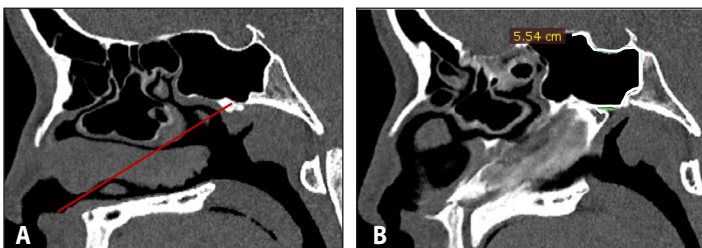


Figure 5. Reconstructive Measurements: **A.** Potential Nasoseptal Flap Length (NSF); and **B.** Potential Sellar Defect Length (SDL)

but align more closely with observations noted by Purcell *et al.*¹⁰ and Ghosh *et al.*²⁵ who demonstrated that NSF was generally sufficient for pediatric sellar reconstruction. One plausible explanation to this is that proportional craniofacial growth preserves relative reconstructive capacity despite dimensional differences. Nonetheless, radiographic feasibility does not necessarily equate to intraoperative ease, and prospective surgical correlation studies are recommended to confirm clinical applicability.

Unlike other studies reporting sex-dependent differences in

parameters such as NSD,^{9,17} our data showed no statistically significant sex-based variations in any anatomical parameter. This finding suggests that sex does not need to be factored into preoperative surgical planning for Filipino pediatric patients, allowing surgeons to focus on age-based anatomical considerations.

Despite the promising findings seen in our study, it is not without limitations. Although the sample size was determined to be statistically adequate based on power analysis for the primary objectives, it may still be considered limited in terms of its ability to support broader generalizations. The limited sample size in the <5 years group, with further subdivision by sex, may reduce statistical power for detecting subtle but clinically meaningful differences within this critical age range. Additionally, infants and very young children (0-2 years) appear to be minimally represented, yet this population would present the most extreme anatomical constraints. Future prospective studies with targeted recruitment to achieve more balanced age distribution, particularly oversampling the <5 years cohort, or more granular age-stratified analyses (e.g., 0-2, 2-5, 5-8, 8-12, 13-17 years), could strengthen the generalizability of our findings.

Second, the retrospective nature of our study is also a limitation, in that the study design may introduce selection bias and limit control over imaging parameters. CT scans were obtained for clinical indications unrelated to skull base pathology rather than for research purposes, potentially introducing referral bias toward certain pathologies or clinical presentations. Imaging parameters (slice thickness, reconstruction algorithms) were not standardized across the study period, which may affect measurement precision. Recommendations for future research include prospective studies with larger age-stratified cohorts to validate these findings and enable more comprehensive anatomical characterization.

Third, our study is also limited by the measurement parameters proposed above. Our research was unable to account for other measurements, such as anterior sellar wall thickness, and the perimeter of the sphenoid sinus done in other studies. Furthermore, our study did not also analyze OFD asymmetry between the right and left sides. While the longer OFD was consistently recorded to reflect the more vulnerable side, this approach may have overlooked potentially significant anatomical variations. OFD asymmetry is clinically relevant, particularly in pediatric EES. Future studies should consider bilateral OFD measurements and quantify asymmetry to better inform surgical risk assessment and planning.

Fourth, the single-center design from a tertiary hospital in Metro Manila limited geographic and socioeconomic generalizability. Regional variations in craniofacial morphology across the Philippine archipelago may exist but were not captured. Multicenter studies



incorporating regional medical centers from different areas (Luzon, Visayas, Mindanao) may provide more comprehensive national normative data.

Fifth, our study did not include functional outcome data or surgical correlation. While we demonstrated that anatomical parameters were measurably different across age groups and that NSR suggested feasibility of reconstruction, we cannot directly correlate these measurements with actual surgical outcomes, complication rates, or long-term functional results in Filipino pediatric patients undergoing EES. Prospective studies with surgical correlation could validate whether these anatomical thresholds translate to clinically meaningful differences in operative difficulty, safety, or outcomes.

Finally, inter-rater and intra-rater reliability of measurements were not formally assessed. While measurements were cross-checked by a radiologist co-author, formal assessment of measurement reproducibility would strengthen confidence in the precision and reliability of the reported values.

Despite these limitations, our study provides the first comprehensive

radiographic analysis of Filipino pediatric skull base anatomy and establishes important baseline data to guide surgical planning. Our findings should be interpreted with awareness of the above limitations, and future multicenter prospective studies with larger, age-balanced cohorts are recommended to validate and extend these results.

In conclusion, our study provides the first radiographic characterization of pediatric skull base anatomy among Filipinos and demonstrates significant age-related changes in key anatomical parameters relevant to EES. Measurements of PAW, NSD, SSD, SW, ICD-SC, ICD-CS, NSF and SDL increased progressively with age, reflecting the ongoing craniofacial development from early childhood to adolescence. Despite smaller absolute anatomical dimensions in younger children, the NSR remained more than 1 across all age groups, suggesting that nasoseptal flap reconstruction is radiographically feasible throughout pediatric development. Our findings provide population-specific anatomical data and highlights that age – rather than sex – should be the primary anatomical consideration in pre-operative planning and surgical decision-making in pediatric EES.

ACKNOWLEDGEMENTS

We appreciate the statistical consultation provided by John Rey B. Macindo, BSN, RGN, RN, MPH, DIH, PStat® (ASA), MAN(c), who assisted with multivariate analysis and interpretation of results.

REFERENCES

- Chivukula S, Koutourousiou M, Snyderman CH, Fernandez-Miranda JC, Gardner PA, Tyler-Kabara EC. Endoscopic endonasal skull base surgery in the pediatric population. *J Neurosurg Pediatr.* 2013 Mar;11(3):227-241. DOI: 10.3171/2012.10.PEDS12160; PubMed PMID: 23240846.
- Mondia MWL, Espiritu AI, Batara JMF, Jamora RDG. Neuro-oncology in the Philippines: a scoping review on the state of medical practice, deterrents to care and therapeutic gaps. *Ecantermedicalscience.* 2021 May 20;15:1238. DOI:10.3332/ecancer.2021.1238; PubMed PMID: 34221121; PubMed Central PMCID: PMC8225337.
- Dusick JR, Esposito F, Mattozo CA, Chaloner C, McArthur DL, Kelly DF. Endonasal transsphenoidal surgery: the patient's perspective—survey results from 259 patients. *Surg Neurol.* 2006 Apr;65(4):332-341. DOI: 10.1016/j.surneu.2005.12.010; PubMed PMID: 16531188.
- Chen J, Pool C, Slonimsky E, King TS, Pradhan S, Wilson MN. Anatomical parameters and growth of the pediatric skull base: endonasal access implications. *J Neurol Surg B Skull Base.* 2022 Jul;84(4):336-348. DOI:10.1055/a-1862-0321; PubMed PMID: 37408579; PubMed Central PMCID: PMC10317570.
- Lenze NR, Gossett KA, Farquhar DR, Quinsey C, Sasaki-Adams D, Ewend MG, et al. Outcomes of endoscopic versus open skull base surgery in pediatric patients. *Laryngoscope.* 2021 May;131(5):996-1001. DOI: 10.1002/lary.29127; PubMed PMID: 33135787.
- LoPresti MA, Sellin JN, DeMonte F. Developmental Considerations in Pediatric Skull Base Surgery. *J Neurol Surg B Skull Base.* 2018 Jan 5;79(1):3-12. DOI:10.1055/s-0037-1617449; PubMed PMID: 29404235; PubMed Central PMCID: PMC5796821.
- Valencia-Sanchez BA, Kim JD, Zhou S, Chen S, Levy ML, Roxbury C, et al. Special considerations in pediatric endoscopic skull base surgery. *J Clin Med.* 2024 Mar 26;13(7):1924. DOI: 10.3390/jcm13071924; PubMed PMID: 38610689; PubMed Central PMCID: PMC11013018.
- Rastatter JC, Walz PC, Alden TD. Pediatric skull base reconstruction: case report of a tunneled temporoparietal fascia flap. *J Neurosurg Pediatr.* 2016 Mar;17(3):371-377. DOI: 10.3171/2015.6.PEDS1588; PubMed PMID: 26544081.
- Tatreau JR, Patel MR, Shah RN, McKinney KA, Wheelless SA, Senior BA, et al. Anatomical considerations for endoscopic endonasal skull base surgery in pediatric patients. *Laryngoscope.* 2010 Sep;120(9):1730-1737. DOI: 10.1002/lary.20964; PubMed Central PMCID: 20717950.
- Purcell PL, Shinn JR, Otto RK, Davis GE, Parikh SR. Nasoseptal flap reconstruction of pediatric sellar defects: a radiographic feasibility study and case series. *Otolaryngol Head Neck Surg.* 2015 Feb 24;152(4):746-751. DOI:10.1177/0194599815571284; PubMed PMID: 25715351; PubMed Central PMCID: PMC10163894.
- Likus W, Gruszczynska K, Markowski J, Machnikowska-Sokolowska M, Olczak Z, Bajor G, et al. Correlations between selected parameters of nasal cavity in neonates and young infants—computed tomography study. *Folia Morphol (Warsz).* 2016;75(3):334-340. DOI: 10.5603/FM.a2015.0128; PubMed PMID: 26711652.
- Shah RN, Surowitz JB, Patel MR, Huang BY, Snyderman CH, Carrau RL, et al. Endoscopic pedicled nasoseptal flap reconstruction for pediatric skull base defects. *Laryngoscope.* 2009 Jun;119(6):1067-1075. DOI: 10.1002/lary.20216; PubMed PMID: 19418531.
- Policina C, Ambrocio GM, Roldan R, Grullo PE. Sinonasal anatomy variations on CT scans of a sample of Filipino adults with chronic rhinosinusitis. *Philipp J Otolaryngol Head Neck Surg.* 2023 Jan-Jun;38(1):22-27. DOI:10.32412/pjohns.v38i1.2139.
- Paber JELB, Cabato MSD, Villarta RL, Hernandez JG. Radiographic analysis of the ethmoid roof based on KEROS classification among Filipinos. *Philipp J Otolaryngol Head Neck Surg.* 2008 Jan-Jun;23(1):15-19. DOI:10.32412/pjohns.v23i1.763.
- Palacios MK, Amable JP, Capio K. Radiologic evaluation of the anterior and posterior ethmoidal foramen and optic canal by paranasal sinus computed tomography scan among adult Filipinos. *Philipp J Otolaryngol Head Neck Surg.* 2022 Jan-Jun;37(1):20-22. DOI:10.32412/pjohns.v37i1.1733.
- Keros P. [On the practical value of differences in the level of the lamina cribrosa of the ethmoid]. *Z Laryngol Rhinol Otol.* 1962 Nov;41:809-813. PubMed PMID: 14032071.
- Sawant N, Sabarish SS, George T, Shivhare P, Sudhir BJ, Kesavadas C, et al. A study of the developing paediatric skullbase anatomy and its application to endoscopic endonasal approaches in children. *Neural India.* 2020 Sep-Oct;68(5):1065-1072. DOI: 10.4103/0028-3886.294543; PubMed PMID: 33109854.
- Hughes DC, Kaduthodil MJ, Connolly DJ, Griffiths PD. Dimensions and ossification of the normal anterior cranial fossa in children. *AJNR Am J Neuroradiol.* 2010 Aug;31(7):1268-1272. DOI: 10.3174/ajnr.A2107; PubMed PMID: 20413607; PubMed Central PMCID: PMC7965475.
- Banu MA, Rathman A, Patel KS, Souweidane MM, Anand VK, Greenfield JP, et al. Corridor-based endonasal endoscopic surgery for pediatric skull base pathology with detailed radioanatomic measurements. *Neurosurgery.* 2014 Jun;10 Suppl 2:273-293. DOI:10.1227/NEU.0000000000000252; PubMed PMID: 24845548.
- Kuan EC, Kaufman AC, Lerner D, Kohanski MA, Tong CCL, Tajudeen BA, et al. Lack of sphenoid pneumatization does not affect endoscopic endonasal pediatric skull base surgery outcomes. *Laryngoscope.* 2019 Apr;129(4):832-836. DOI:10.1002/lary.27600; PubMed PMID: 30520033.
- Özer CM, Atalar K, Öz II, Toprak S, Barut Ç. Sphenoid sinus in relation to age, gender, and cephalometric indices. *J Craniofac Surg.* 2018 Nov;29(8):2319-2326. DOI:10.1097/SCS.0000000000004869; PubMed PMID: 30320684.
- Nair S, Ibrahim A. The importance of cribriform-lamella angle in endoscopic sinus surgery. *Indian J Otolaryngol Head Neck Surg.* 2020 Sep 26;73(1):66-71. DOI:10.1007/s12070-020-02171-7; PubMed PMID: 33643886; PubMed Central PMCID: PMC7881950.
- Güven M, Elden H, Yaylacı A, Güven EM, Kara A, Orha AT. Age-dependent differences of the depth of olfactory fossa in children. *Brazilian J Otorhinolaryngol.* 2022 Nov-Dec;88 Suppl 5(Suppl 5):S52-S56. DOI: 10.1016/j.bjorl.2021.09.006; PubMed PMID: 34799268; PubMed Central PMCID: PMC9801024.
- Wu T, Chandy Z, Ference E, Lee JT. Endoscopic skull base surgery in the pediatric population. *Curr Treat Options Allergy.* 2021 May;8:274-284. DOI:10.1007/s40521-021-00288-w.
- Ghosh A, Hatten K, Learned KO, Rizzi MD, Lee JY, Storm PB, Palmer JN, Adappa ND. Pediatric nasoseptal flap reconstruction for suprasellar approaches. *Laryngoscope.* 2015 Nov;125(11):2451-6. DOI: 10.1002/lary.25395; PubMed PMID: 26016422.